Preparation of glass-based composites with green upconversion and persistent luminescence using modified direct doping method

V. Lahti [a,*], N. Ojha [a], S. Vuori [b,c], M. Lastusaari [b,d], L. Petit [a]

[a] Photonics Laboratory, Tampere University, FI-33101, Tampere, Finland
[b] University of Turku, Department of Chemistry, FI-20014, Turku, Finland
[c] University of Turku Graduate School (UTUGS), Doctoral Programme in Physical and Chemical Sciences, FI-20014, Turku, Finland
[d] Turku University Centre for Materials and Surfaces (MatSurf), Turku, Finland

HIGHLIGHTS

- New glasses were prepared using direct doping process.
- Adding persistent luminescent particles doesn't impact $Er:CaF_2$ crystal precipitation.
- Direct doping process needs to be modified to limit the evaporation of fluorine.
- The new composite exhibits green upconversion and green persistent luminescence.

ABSTRACT

New oxyfluorophosphate glass-based composites which exhibit not only green upconversion under 980 nm pumping but also green persistent luminescence (PeL) after being UV charged were successfully prepared using the direct doping method. The composites are composed of a glass-ceramic with Er^{3+} doped CaF_2 crystals and of the persistent luminescent particles with the $SrAl_2O_4:Eu,Dy$ composition. In the standard direct doping method, the glass melt is quenched few minutes after adding the PeL particles in the melt held at a temperature lower than the melting temperature. It is demonstrated that the direct doping method should be modified when preparing oxyfluoride glasses with PeL particles to limit not only the decomposition of the PeL particles in the glass but also the fluorine evaporation occurring during the glass preparation. Here, the composites were prepared by quenching the melt right after adding the PeL particles. The modified direct doping method allows the preparation of glass-based composites with strong green upconversion and homogeneous green persistent luminescence.

1. Introduction

Since the discovery of the first modern persistent luminescent (PeL) phosphors such as $SrAl_2O_4:Eu^{2+},Dy^{3+}$ [1], $CaAl_2O_4:Eu^{2+},Nd^{3+}$ [2], $Sr_4Al_{14}O_{24}:Eu^{2+},Dy^{3+}$ [3] and $Sr_2MgSi_2O_7:Eu^{2+},Dy^{3+}$ [4], materials with persistent luminescence have been materials of interest as they can find multiple applications in interior decorations, night vision, displays, signals, anti-counterfeiting, optical recording, or biochemistry, just to cite few applications [5]. Persistent luminescence is an emission which can last for a long time (from seconds to hours) after removing the irradiation source [6,7]. The longest visible PeL was achieved by introducing Dy^{3+} in the $SrAl_2O_4:Eu^{2+}$ [8] with already a relatively long-lasting afterglow [9].

Glass-based materials with persistent luminescence were obtained using heat-treatment [10]. The persistent luminescence was achieved due to the precipitation of $SrAl_2O_4:Eu,Dy$ crystals in the glass during the heat treatment. Glasses with PeL were also prepared using the direct doping method, the technique of which is explained in Ref. [11]. In this method, the particles are added in the glass melt after the melting. The doping temperature (T_{doping}), defined as the temperature at which the particles are added in the melt, is lower than the melting temperature and needs to be optimized for homogeneous dispersion of the particles in the glass. The particles should be thermally stable at this doping temperature, so they don't decompose in the glass during the glass

---

* Corresponding author.
  E-mail address: vilma.s.lahti@tuni.fi (V. Lahti).

preparation. However, as explained in Ref. [12], decomposition of the PeL particles always occurs during the glass preparation leading to a degradation in their PeL properties despite the optimization of the doping temperature. The decomposition of the particles was, also, found to depend on the corrosive behavior of the glass melt [13]. Nonetheless, a large variety of PeL glasses with various compositions has been prepared over the past few years using the direct doping method [12–14].

Recently, particles with green PeL have been combined with rare-earth ions to prepare NIR rechargeable "optical battery" which generates green PeL after 980 nm pumping [15]. This was achieved by combining crystals with typical UV/blue upconversion emission (350/475 nm) such as $NaYF_4$:Yb,Tm and the $SrAl_2O_4$:Eu,Dy persistent luminescent particles. Because of the overlapping between the UV/blue upconversion emission and the absorption of the persistent phosphors, the 980 nm NIR excitation can be used to active the green persistent luminescence at ~520 nm. Additionally, upconverter materials have found applications in solar cell. As the energy of the solar IR light is lower than the bandgap energy of the typical solar cell, about half of the total solar energy flux in the infrared is lost due to thermalization and non-absorption. As upconverter materials can be used to convert a NIR light into visible light through multiphoton processes [16], enhancement of the power conversion efficiencies (PCEs) of solar cells has been reported in many studies when inserting such upconverters in the cell [17,18]. Therefore, upconverter materials which contain also PeL particles are of great interest for the development of new optical batteries or solar cells for example.

The Er^{3+} doped $75NaPO_3$–$25CaF_2$ (in mol%) glass was reported to be a promising glass as transparent glass-ceramics with intense green upconversion under 980 nm pumping can be prepared from this glass after heat-treatment. The green upconversion is due to the precipitation of Er^{3+} doped CaF_2 crystals in the volume of the glass during the heat treatment [19]. Indeed, CaF_2 nanocrystals have been of great interest as host for rare-earth ions [20] due to their low phonon energy which lead to strong upconversion emission from the rare-earth ions [21]. However, the preparation of this glass is challenging as this glass contains fluorine, known to be a volatile element [22]. Indeed, it was reported that the evaporation of fluorine increases the glass crystallization tendency and limits the volume precipitation of Er^{3+} doped CaF_2 crystals in the glass with the composition $75NaPO_3$–$25CaF_2$ (in mol%) [19]. This glass was prepared with PeL particles using the direct doping method [23]. However, crystallization occurred during quenching. The crystallization was associated with the evaporation in fluorine taking place during the glass preparation, mainly due to the use of quartz crucible.

Here, a study on the preparation of Er^{3+} doped glass-based composite in the $NaPO_3$–CaF_2 system with persistent luminescence is reported. In this study, Pt crucible is used to limit the evaporation of fluorine during the glass melting. The impact of the direct doping process on the nucleation and growth of Er^{3+} doped crystals in the glass is discussed.

2. Experimental

Glasses with the composition $74.81NaPO_3$ – $24.94CaF_2$ – $0.25Er_2O_3$ were prepared with 0.5 wgt% of the commercial $SrAl_2O_4$:Eu^{2+},Dy^{3+} persistent luminescent (PeL) particles (MPs) using the direct doping method. The raw materials were $(NaPO_3)_6$ (Alfa Aesar, tech.), CaF_2 (Alfa Aesar, 99.95%) and Er_2O_3 (Aldrich, ≥99.95%). They were mixed and grinded in a mortar prior to the melting. The glasses were melted at 950 °C for 5 min in platinum (Pt) crucible. The temperature of the melt was reduced to the doping temperature (825, 875 and 900 °C) prior to adding the PeL particles in the glass melt. The glasses were quenched 3 min after adding the particles and finally annealed for 4 h at 200 °C. After the annealing, the glasses were heat-treated. The glasses were placed on a platinum foil to prevent contamination from the sample holder.

The thermal properties of the glasses were measured using differential thermal analysis (DTA) (TA instruments SDT Q600) using a Pt pan, N_2 atmosphere and 10 °C/min heating rate. The glass transition temperature (T_g) was taken at the inflection point of the endotherm, the crystallization temperature (T_p) at the maximum of the exothermic peak and T_x at the onset of the crystallization peak. The accuracy of the measurement is ±3 °C.

The composition of the PeL particles in the glasses was analyzed using a scanning electron microscope (Carl Zeiss Crossbeam 540) equipped with Oxford Instruments X-Max^N 80 EDS detector. Prior to the measurement, a thin carbon layer was deposited at the surface of the glasses. The accuracy of the elemental analysis is ±1.5 mol%.

An Electron Probe MicroAnalyzer (EPMA) coupled with a wave-length dispersive X-Ray analyzer (WDX) was used to determine the fluorine content with an accuracy of ±0.1 at %.

The XRD analysis was carried out on powder samples with the Panalytical EMPYREAN multipurpose X-Ray Diffractometer using nickel filtered copper K-Alpha radiation. The spectra were obtained using the Bragg-Brentano geometry and rotating the sample holder around the Phi-axis at a constant speed of 16 revolutions per minute.

The upconversion spectra of the glasses were measured on samples crushed into powder at room temperature using a Spectro 320 optical spectrum analyzer (Instrument Systems Optische Messtechnik GmbH, Germany). The center emission wavelength (λ_{exc}) of the laser was ~975 nm and its incident power at the sample surface was ~23.5 mW.

A Varian Cary Eclipse Fluorescence Spectrophotometer equipped with a Hamamatsu R928 photomultiplier (PMT) was used to collect the persistent luminescence (PeL) spectra of the PeL glasses, crushed into powder for the analysis. After 5 min of irradiation with a compact UV lamp (UVGL-25, 4 W, λ_{exc}: 254 nm), the PeL spectra were measured 1 min after ceasing the irradiation using a data collection time of 4 s for the whole spectrum. The photoluminescence (PL) spectra were measured using a pulsed Nd:YAG laser (λ_{exc}: 266 nm, 8 ns, TII Lotis) using a CCD camera (Avantes, AvaSpec-HS-TEC). All spectra were measured at room temperature.

The reflectance spectrum of the as-prepared glass was measured with Avantes AvaSpec ULS2048CL-EVO spectrometer coupled with an Avantes FC-IR600-1-ME-HTX optical fiber. The light source was an Ocean Optics LS-1 Cal calibration lamp directed towards the sample 20 cm away.

3. Results and discussion

The direct doping method was used to prepare new Er^{3+} doped PeL glasses in the $NaPO_3$– CaF_2 system. The doping temperature was varied between 825 and 900 °C in order to prepare amorphous glasses while ensuring the survival and dispersion of the PeL particles in the glass as performed in Refs. [12–14]. One should remind that T_{doping} should be lower than the melting temperature to limit the decomposition of the particles but not too low as the viscosity of the melt increases as the T_{doping} decreases.

As seen in Fig. 1, the as-prepared glasses remain translucent as compared to the glasses obtained using quartz crucible [23].

As opposed to our previous study [23], the newly developed glasses were prepared in Pt crucible to limit the fluorine losses. As reported in Table 1, the loss in F is expected to be 44% when using a T_{doping} of 900 °C whereas a fluorine loss of 93 at % was reported when prepared using the same T_{doping} in quartz crucible. According to Ref. [24], the large loss in F when using quartz crucible is due to the formation of SiF_4 gas molecules due to the chemical reaction between CaF_2 and SiO_2.

All the newly developed glasses exhibit green afterglow after UV charging confirming the presence of PeL particles in the glasses. However, the glasses exhibit inhomogeneous PeL due to aggregates of the PeL particles in the glasses. The intensity of the afterglow was found to decrease as the T_{doping} increases as seen in Fig. 1a. As explained in our previous studies [12–14], the decrease in the PeL can be related to the decomposition of the PeL particles occurring during the glass melting.
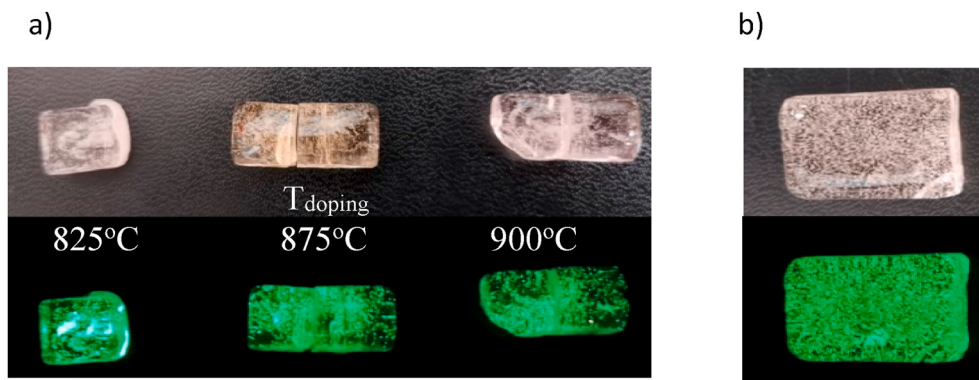
a)

b)

Fig. 1. Pictures in daylight and after stopping the UV irradiation of the glasses prepared by adding the PeL particles at different doping temperatures (T_{doping}) (a) and of the glass prepared by adding the PeL particles at 950 °C before quenching the melt (b).

Table 1
Fluorine content in the investigated glasses and their thermal properties.

Samples	Expected F at %	Measured F at % (±0.1 at %)	% loss of F	T_g ±3 (°C)	T_x ±3 (°C)	T_p ±3 (°C)	ΔT (T_x-T_g) ±6 (°C)
PeL particles free glass	11.1	9.1	18	269	323	338	54
PeL particles added at 950 °C		9.0	19	275	336	352	61
T_{doping} = 825 °C		6.7	40	281	350	422	69
T_{doping} = 875°C		6.3	43	288	373	448	85
T_{doping} = 900°C		6.2	44	291	376	461	85

Thus, decomposition of the PeL particles is expected when preparing a glass with a high T_{doping}. Fig. 2a and b exhibit the PeL and PL spectra of the glasses, respectively.

The PeL spectra exhibit two bands while the spectrum of the PeL particles alone depicts only one band which can be related to the $4f^6 5 d^1$ → $4f^7$ transition of Eu^{2+} ions located in one site in the $Sr_4Al_{14}O_{25}$ structure [25]. The apparent presence of the 2 bands is mostly due to the self-absorption of the glasses as they absorb at 520 nm due to the Er^{3+} ions. The shape of the PL band remains unchanged after embedding the PeL particles in the glass, except at 620 nm; the intensity of the shoulder increases after adding the PeL particles in the glass. This emission band at 620 nm can be associated with the emission from Eu^{3+} ions [26]. Therefore, some Eu^{2+} are thought to oxidize into Eu^{3+} confirming the partial decomposition of the PeL particles happening during the melting process as seen in other PeL glasses [12–14].

The partial decomposition of the particles was evidenced using SEM. The composition analysis performed across a particle found at the surface of the glasses clearly shows that the PeL particles maintain, in their center, their composition confirming the $SrAl_2O_4$ composition (see Fig. 3). However, as the T_{doping} temperature increases, the PeL particles exhibit an outermost layer which is Al rich compared to the inner part. Similar Al rich outer layer at the interface with the glass was reported in Ref. [27] and was related to the decomposition of the particles; the larger T_{doping}, the larger amount of Al in the outermost layer. According to the composition analysis, the PeL particles are not suspected to degrade in the glass when using a T_{doping} of 825 °C. More importantly, crystals can be seen at the PeL particles – glass interface. According to the composition analysis, they appear to be P and Ca rich crystals. One
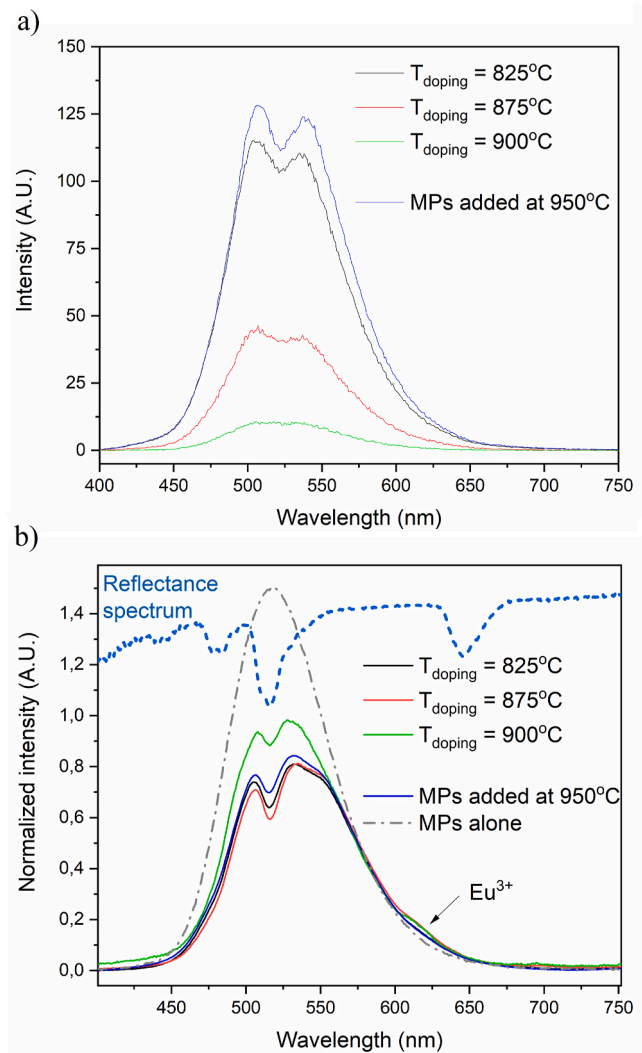
a)

b)

Fig. 2. Persistent Luminescence (PeL) (a) and normalized conventional luminescence (PL) (b) spectra of the investigated glasses measured at room temperature. Also shown in b) are the PL spectrum of the PeL particles alone (MPs alone) and the reflectance spectrum of the glass. The PL intensities in b) were normalized to account for the self-absorption for comparison purposes.

should mention that a heat-treatment of the Er^{3+} doped $75NaPO_3$–$25CaF_2$ glass led to the precipitation of similar crystals [28, 29]. It is interesting to point out that the number and size of the crystals
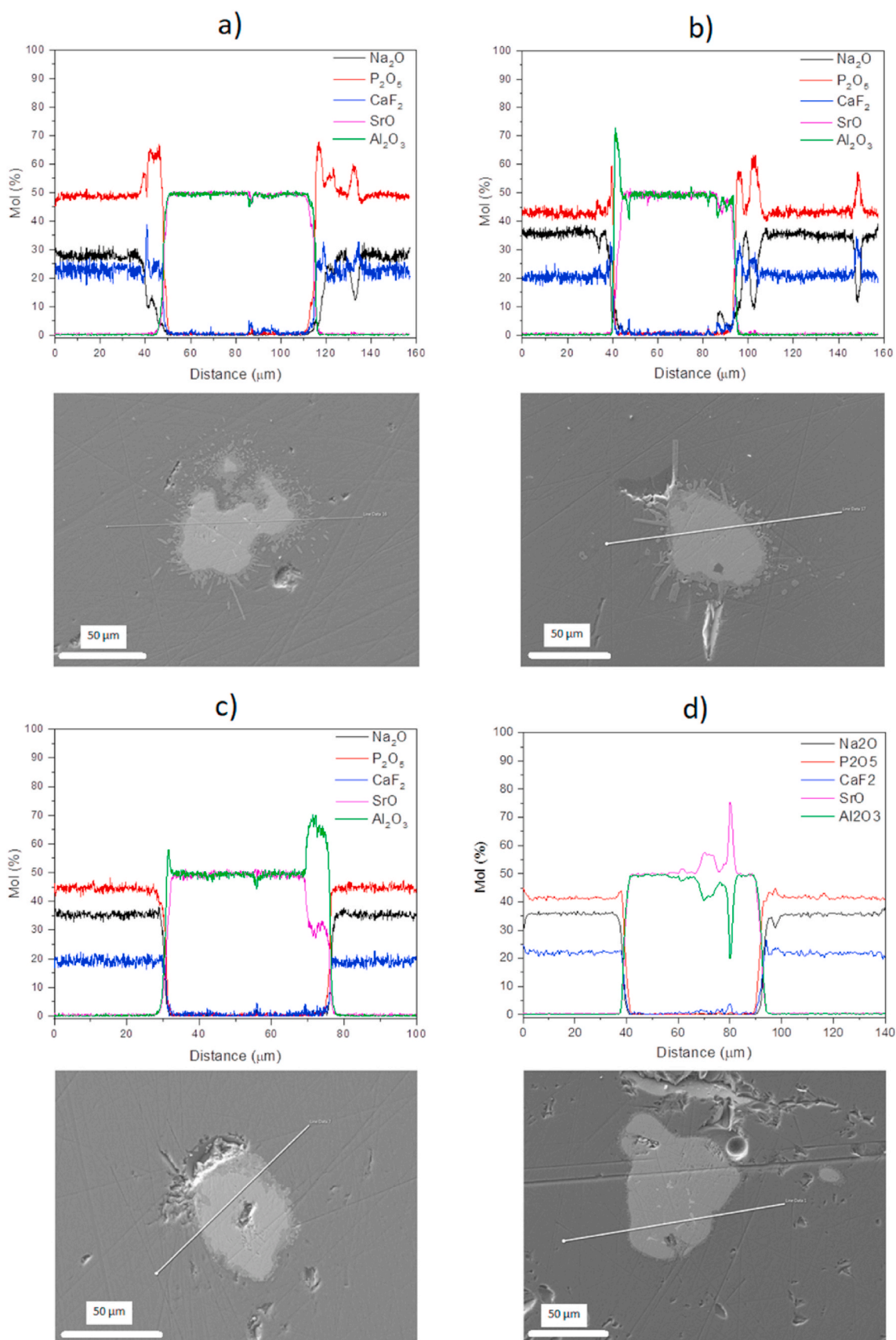
Fig. 3. SEM/EDS line profiles giving the elemental distribution across a PeL particle found at the surface of the glasses prepared at T_{doping} of 825 °C (a), 875 °C (b), 900 °C (c) and by adding the PeL particles at 950 °C (d).

depend on the T_{doping}. As a large amount of crystals can be seen around the particles when preparing the glass using a T_{doping} of 825 °C, the precipitation of the crystals cannot be related to the partial decomposition of the PeL particles. Therefore, the PeL particles are thought to act as nucleation agents leading to heterogeneous nucleation. Nonetheless, as shown in Fig. 1, the glasses appear transparent despite the precipitation of these small crystals at the PeL particles-glass interface. One should mention no peaks were seen in the XRD pattern of the glasses indicating that the P and Ca rich crystals around the PeL particles are probably too small and/or too few to be detected using XRD.

As performed in Ref. [19,29], the glasses were heat-treated at $(T_g+20 °C)$ for 17 h and at T_p for 1 h using the thermal properties of the glasses reported in Table 1. The heat-treated glasses became translucent confirming crystallization as evidenced using XRD. The XRD patterns of the heat-treated glasses are shown in Fig. 4. Surprisingly, they exhibit peaks which can be related not only to CaF_2 but also to $NaPO_3$ and $Na_2Ca_2P_2O_7F_2$ crystals.

It was recently demonstrated in Ref. [28] that an increase in the growth temperature during the heat-treatment of glasses in the $NaPO_3$–CaF_2 system leads to the precipitation of $NaPO_3$ and $Na_2Ca_2P_2O_7F_2$ at the expense of CaF_2 crystals. Thus, the crystallization of other crystals than CaF_2 in the investigated heat-treated glasses needs to be related to the temperature used for the heat treatment. Indeed, an increase in T_{doping} increases T_g, T_x and T_p due to the evaporation of the fluorine during the melting process as evidenced using EPMA (see Table 1). To avoid the crystallization of other crystals than CaF_2, the PeL glasses were heat-treated at $(T_g+20 °C)$ for 17 h and for 1 h at 330 °C, the T_p of the glass prepared using standard melting process at which CaF_2 is the only crystal phase which precipitates in the glass matrix. The XRD pattern of these heat-treated glasses exhibit few peaks which can be related only to CaF_2 crystals (See Fig. 4). This clearly shows that the addition of PeL particles in the $NaPO_3$–CaF_2 glass system and their partial decomposition have no significant impact on the nucleation and growth of the CaF_2 crystals.

The upconversion spectra of the PeL glasses after heat-treatment are shown in Fig. 5a.

The spectra exhibit the typical green and red emissions from the Er^{3+} ions. An increase in the intensity of the upconversion was observed after heat-treatment confirming the precipitation of Er^{3+} ions in the CaF_2 crystals as the up-conversion process between Erbium ions is favored by
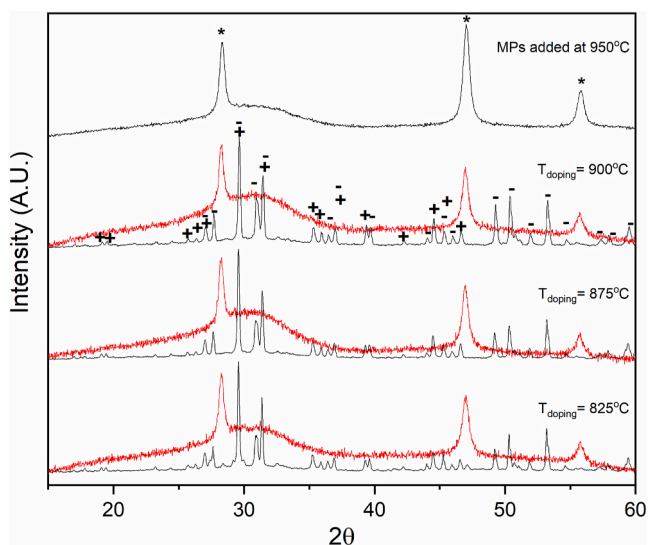

Fig. 4. XRD pattern of the investigated glasses after heat-treatment at $(T_g+20 °C)$ for 17 h and at T_p for 1 h (black) and at $(T_g+20 °C)$ for 17 h and at 330 °C for 1 h (red). (+$NaPO_3$, -$Na_2Ca_2P_2O_7F_2$ and * CaF_2 crystals). (For interpretation of the references to colour in this figure legend, the reader is referred to the Web version of this article.)
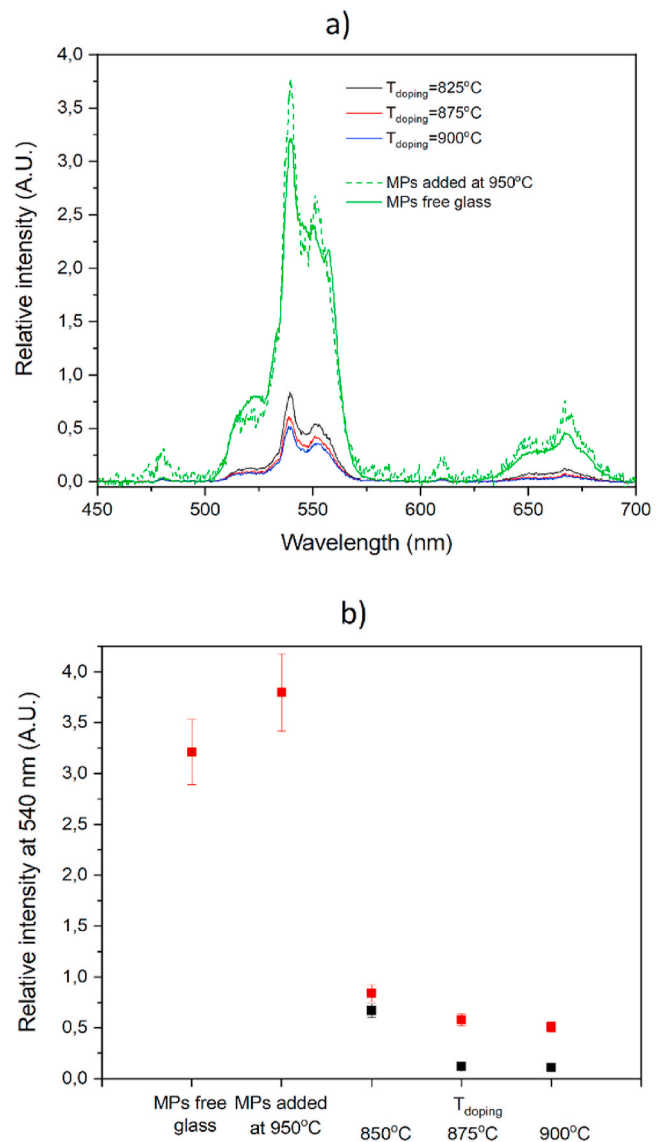

Fig. 5. Upconversion spectra of the investigated glasses after heat-treatment at $(T_g+20 °C)$ for 17 h and at 330 °C for 1h (a) and Relative intensity of the emission at 540 nm (b) of the investigated glasses after heat-treatment at $(T_g+20 °C)$ for 17 h and at T_p for 1 h (black) and at $(T_g+20 °C)$ for 17 h and at 330 °C for 1 h (red). (For interpretation of the references to colour in this figure legend, the reader is referred to the Web version of this article.)

the low phonon energy of the CaF_2 crystals as explained in Ref. [28]. However, as shown in Fig. 5b, the intensity of the upconversion from the heat-treated PeL glasses is smaller than from the heat-treated PeL free glass due to the low amount of F in the PeL glasses. Indeed, a lower amount of Er^{3+} doped CaF_2 crystals are expected in the PeL glasses compared to the PeL free glasses. One should mention that the crystallization has no significant impact on the PeL and PL properties of the PeL particles (not shown here).

In order to limit the evaporation of fluorine during the preparation of the PeL glasses, the direct doping method was modified. A PeL glass was prepared by adding the PeL particles in the glass melt after the melting at 950 °C and before quenching the glass. To guarantee the homogenous dispersion of the PeL particles, the glass melt was vigorously stirred prior to the quenching. This glass is referred as PeL particles added at 950 °C (MPs added at 950 °C). As shown in Fig. 1b, the glass exhibits also homogeneous PeL. The PeL and PL spectra of this glass are similar to the spectra of the glass prepared using a T_{doping} of 825 °C indicating that

limited decomposition of the PeL particles occurred in this glass as confirmed using SEM (Fig. 3d) although the temperature of the melt was 950 °C. The limited decomposition of the PeL particles is due to the short melting process as the glass was quenched after adding the PeL particles. By reducing the duration of the glass melting process, the glass exhibits similar loss in F and thus similar thermal properties than the glass prepared using standard melting process (Table 1). As for the other PeL glasses, this glass was heat-treated at (T_g+20 °C) for 17 h and at T_p for 1 h. Its XRD pattern exhibits only the peaks related to CaF_2 crystals (Fig. 4). Finally, and more importantly, due to the low loss in F during the glass preparation, this heat-treated PeL glass exhibits higher intensity of upconversion compared to the other PeL glass-ceramic (Fig. 5), the intensity of the upconversion from this glass being actually similar to the intensity of the PeL free glass.

4. Conclusion

In summary, new PeL glass-based composites were successfully prepared with green upconversion under 980 nm pumping and also with green persistent luminescence (PeL) after UV charging. This was achieved by adding $SrAl_2O_4$:Eu^{2+},Dy^{3+} persistent luminescent (PeL) particles in the glass melt. We clearly explain all the challenges related to the preparation of oxyfluorophosphate glass-based composite. The direct doping method had to be modified to limit the evaporation of fluorine during the glass melting. We demonstrate that it is possible to add the PeL particles in the glass at the melting temperature prior to the quenching not only to limit the decomposition of the PeL particles but also to limit the fluorine evaporation. This modified direct doping method allows the preparation of oxyfluorophosphate glass-based composite with strong green upconversion and with homogeneous green PeL.

Credit author statement

L.P. and M.L. conceived and designed this work. V.L. and N.O. prepared and characterized the glasses while S.V. carried out the measurement of the PeL and PL properties. L.P. wrote the original draft. All the authors discussed the results and contributed to the writing of the manuscript. All authors have read and agreed to the published version of the manuscript.

Declaration of competing interest

The authors declare that they have no known competing financial interests or personal relationships that could have appeared to influence the work reported in this paper.

References

[1] T. Matsuzawa, Y. Aoki, N. Takeuchi, Y. Murayama, A new long phosphorescent phosphor with high brightness, $SrAl_2O_4$: Eu^{2+} , Dy^{3+}, J. Electrochem. Soc. 143 (1996) 2670–2673, https://doi.org/10.1149/1.1837067.

[2] T. Katsumata, T. Nabae, K. Sasajima, T. Matsuzawa, Growth and characteristics of long persistent $SrAl_2O_4$- and $CaAl_2O_4$-based phosphor crystals by a floating zone technique, J. Cryst. Growth 183 (1998) 361–365, https://doi.org/10.1016/S0022-0248(97)00308-4.

[3] Y. Lin, Z. Tang, Z. Zhang, Preparation of long-afterglow $Sr_4Al_{14}O_{25}$-based luminescent material and its optical properties, Mater. Lett. 51 (2001) 14–18, https://doi.org/10.1016/S0167-577X(01)00257-9.

[4] Y. Lin, Z. Tang, Z. Zhang, X. Wang, J. Zhang, Preparation of a new long afterglow blue-emitting $Sr_2MgSi_2O_7$-based photoluminescent phosphor, J. Mater. Sci. Lett. 20 (2001) 1505–1506, https://doi.org/10.1023/A:1017930630889.

[5] Z. Pan, Y.-Y. Lu, F. Liu, Sunlight-activated long-persistent luminescence in the near-infrared from Cr^{3+}-doped zinc gallogermanates, Nat. Mater. 11 (2012) 58–63, https://doi.org/10.1038/nmat3173.

[6] T. Aitasalo, J. Holsa, H. Jungner, M. Lastusaari, J. Niittykoski, Thermoluminescence study of persistent luminescence Materials: Eu^{2+}- and r^{3+}-doped calcium aluminates, $CaAl_2O_4$:Eu^{2+},R^{3+}, J. Phys. Chem. B 110 (2006) 4589–4598, https://doi.org/10.1021/jp057185m.

[7] T. Maldiney, A. Lecointre, B. Viana, A. Bessiere, M. Bessodes, D. Gourier, C. Richard, D. Scherman, Controlling electron trap depth to enhance optical properties of persistent luminescence nanoparticles for in vivo imaging, J. Am. Chem. Soc. 133 (2011) 11810–11815, https://doi.org/10.1021/ja204504w.

[8] H. Takasaki, S. Tanabe, T. Hanada, Long-lasting afterglow characteristics of Eu, Dy codoped $SrO-Al_2O_3$ phosphor, T. J. Ceram. Soc. Jpn. 104 (1996) 322–326, https://doi.org/10.2109/jcersj.104.322.

[9] V. Abbruscato, Optical and electrical properties of $SrAl_2O_4$:Eu^{2+}, J. Electrochem. Soc. 118 (1971) 930–933, https://doi.org/10.1149/1.2408226.

[10] T. Nakanishi, Y. Katayama, J. Ueda, T. Honma, S. Tanabe, T. Komatsu, Fabrication of Eu:$SrAl_2O_4$-based glass ceramics using Frozen sorbet method, J. Ceram. Soc. Jpn. 119 (2011) 609–615, https://doi.org/10.2109/jcersj2.119.609.

[11] J. Zhao, X. Zheng, E.P. Schartner, P. Ionescu, R. Zhang, T.-L. Nguyen, D. Jin, H. Ebendorff-Heidepriem, Upconversion nanocrystal-doped glass: a new paradigm for photonic materials, Adv. Optical Mater. 4 (2016) 1507–1517, https://doi.org/10.1002/adom.201600296.

[12] N. Ojha, H. Nguyen, T. Laihinen, T. Salminen, M. Lastusaari, L. Petit, Decomposition of persistent luminescent microparticles in corrosive phosphate glass melt, Corrosion Sci. 135 (2018) 207–214, https://doi.org/10.1016/j.corsci.2018.02.050.

[13] N. Ojha, T. Laihinen, T. Salminen, M. Lastusaari, L. Petit, Influence of the phosphate glass melt on the corrosion of functional particles occurring during the preparation of glass-ceramics, Ceram. Int. 44 (2018) 11807–11811, https://doi.org/10.1016/j.ceramint.2018.03.267.

[14] P. Roldán Del Cerro, H. Teittinen, M. Lastusaari, L. Petit, J. Massera, Novel borosilicate bioactive scaffolds with persistent luminescence, Biomed. Glasses 6 (2020) 1–9, https://doi.org/10.1515/bglass-2020-0001.

[15] L. Hu, P. Wang, M. Zhao, L. Liu, L. Zhou, B. Li, F.H. Albaqami, A.M. El-Toni, X. Li, Y. Xie, X. Sun, F. Zhang, Near-infrared rechargeable "optical battery" implant for irradiation-free photodynamic therapy, Biomaterials 163 (2018) 154–162, https://doi.org/10.1016/j.biomaterials.2018.02.029.

[16] T. Trupke, M.A. Green, P. Würfel, Improving solar cell efficiencies by up-conversion of sub-band-gap light, J. Appl. Phys. 92 (2002) 4117–4122, https://doi.org/10.1063/1.1505677.

[17] J. Wu, J. Wang, J. Lin, Z. Lan, Q. Tang, M. Huang, Y. Huang, L. Fan, Q. Li, Z. Tang, Enhancement of the photovoltaic performance of dye-sensitized solar cells by doping $Y_{0.78}Yb_{0.20}Er_{0.02}F_3$ in the photoanode, Adv. Energy Mater. 2 (2012) 78–81, https://doi.org/10.1002/aenm.201100531.

[18] H. Lian, Z. Hou, M. Shang, D. Geng, Y. Zhang, J. Lin, Rare earth ions doped phosphors for improving efficiencies of solar cells, Energy 57 (2013) 270–283, https://doi.org/10.1016/j.energy.2013.05.019.

[19] A. Szczodra, A. Mardoukhi, M. Hokka, N.G. Boetti, L. Petit, Fluorine losses in Er^{3+} oxyfluoride phosphate glasses and glass-ceramics, J. Alloys Compd. 797 (2019) 797–803, https://doi.org/10.1016/j.jallcom.2019.05.151.

[20] D.N. Rao, J. Prasad, P.N. Prasad, Two-photon excitation of Ho^{3+} in the CaF_2, SrF_2, and CdF_2 lattices P, Phys. Rev. B 28 (1983) 20, https://doi.org/10.1103/PhysRevB.28.20.

[21] R.X. Yan, Y.D. Li, Down/up conversion in Ln^{3+}-doped YF_3 nanocrystals, Adv. Funct. Mater. 15 (2005) 763, https://doi.org/10.1002/adfm.200305044.

[22] D. Kumar, R.G. Ward, D.J. Williams, Effect of fluorides on silicates and phosphates, Discuss. Faraday Soc. 32 (1961) 147–154, https://doi.org/10.1039/DF9613200147.

[23] A. Szczodra, L. Kuusela, I. Norrbo, A. Mardoukhi, M. Hokka, M. Lastusaari, L. Petit, Successful preparation of fluorine containing glasses with persistent luminescence using the direct doping method, J. Alloys Compd. 787 (2019) 1260–1264, https://doi.org/10.1016/j.jallcom.2019.02.075.

[24] A.I. Zaitsev, A.V. Leites, A.D. Litvina, B.M. Mogutnov, Investigation of the mould powder volatiles during continuous casting, Steel Res. 65 (1994) 368, https://doi.org/10.1002/srin.199401179.

[25] H. Yamamoto, T. Matsuzawa, Mechanism of long phosphorescence of $SrAl_2O_4$:Eu^{2+},Dy^{3+} and $CaAl_2O_4$:Eu^{2+},Nd^{3+}, J. Lumin. 72–74 (1997) 287–289, https://doi.org/10.1016/S0022-2313(97)00012-4.

[26] K. Sinha, B. Pearson, S.R. Casolco, J.E. Garay, O.A. Graeve, Synthesis and consolidation of $BaAl_2Si_2O_8$:Eu: development of an integrated process for luminescent smart ceramic materials, J. Am. Ceram. Soc. 92 (11) (2009) 2504–2511, https://doi.org/10.1111/j.1551-2916.2009.03242.x.

[27] J. Massera, M. Gaussiran, P. Głuchowski, M. Lastusaari, L. Hupa, L. Petit, Processing and characterization of phosphate glasses containing $CaAl_2O_4$:Eu^{2+},Nd^3

$^+$ and SrAl$_2$O$_4$:Eu^{2+},Dy^{3+} microparticles, J. Eur. Ceram. Soc. 35 (14) (2015) 3863–3871, https://doi.org/10.1016/j.jeurceramsoc.2015.06.031.

[28] N. Ojha, A. Szczodra, N.G. Boetti, J. Massera, L. Petit, Nucleation and growth behavior of Er^{3+} doped oxyfluorophosphate glasses, RSC Adv. 10 (2020) 25703, https://doi.org/10.1039/D0RA04681G.

[29] A. Nommeots-Nomm, N.G. Boetti, T. Salminen, J. Massera, M. Hokka, L. Petit, Luminescence of Er^{3+} doped oxyfluoride phosphate glasses and glass-ceramics, J. Alloys Compd. 751 (2018) 224–230, https://doi.org/10.1016/j.jallcom.2018.04.101.